

Inhibition Effects Of Some Novel Surfactants Based On Corn Oil And Diethanolamine On Mild Steel Corrosion In Chloride Solutions Saturated With CO₂

I. T. Ismayilov¹, Hany M. Abd El-Lateef^{1,2*}, V. M. Abbasov¹, L. I. Aliyeva¹, E. E. Qasimov¹, E. N. Efremenko³, T. A. Ismayilov¹, S. A. Mamedxanova¹

¹Mamedaliev Institute of Petrochemical Processes, National Academy of Sciences of Azerbaijan, AZ1025 Baku, Azerbaijan

²Chemistry Department, Faculty of Science, Sohag University, 82524 Sohag, Egypt

³Faculty of Chemistry, Lomonosov Moscow State University, 119991, GSP-1, 1-3 Leninskiye Gory, Moscow, Russia

*Email: Hany_shubra@yahoo.co.uk

Received: 14 Feb. 2013, Revised: 3 Mar. 2013; Accepted: 19 Mar. 2013

Published online: 1 May 2013

Abstract: Novel surfactants were synthesized based on corn oil and diethanolamine and its inhibiting action on the corrosion of mild steel in CO₂-saturated NaCl solutions was investigated by means of linear polarization resistance corrosion rate and polarization methods. The results revealed that the investigated surfactants were an excellent inhibitors and the inhibition efficiencies obtained from two methods were in good agreement. The maximum inhibition efficiency was observed for inhibitor II (99.5 at 50 ppm). Polarization studies clearly revealed that the surfactants acted essentially as the mixed-type inhibitor. Thermodynamic parameters were obtained from polarization studies, which suggested that the adsorption of studied surfactants on metal surface obeyed Langmuir adsorption isotherm model.

Keywords: surfactants, mild steel, Polarization, inhibition.

1. Introduction

Mild steel is widely applied as the constructional material in many industries due to its excellent mechanical properties and low cost. As some of the important fields of application are petrochemical processes, the main problem of applying mild steel is CO₂ corrosion. Several methods are present for corrosion prevention. One of such methods is the use of the organic inhibitors [1–6]. The use of inhibitors is the most economical and practical method in reducing corrosive attack on metals [7, 8]. Inhibitors which reduce corrosion on metallic materials can be divided into four kinds: (i) inorganic inhibitors, (ii) organic inhibitors, (iii) surfactant inhibitors, and (iv) mixed material inhibitors. Surfactant inhibitors have many advantages such as, for example, high inhibition efficiency, low price, low toxicity, and easy production.

Surfactants are molecules composed of a polar hydrophilic group, the “head”, attached to a nonpolar hydrophobic group, the “tail”. In general, in aqueous solution the inhibitory action of surfactant molecules may also be due to physical (electrostatic) adsorption or chemisorption onto the metallic surface,

depending on the charge of the solid surface and the free energy change of transferring a hydrocarbon chain from water to the solid surface. The adsorption of a surfactant markedly changes the corrosion resisting property of a metal, and for these reasons studies of the relation between adsorption and corrosion inhibition are of considerable importance [9–12]. In corrosion inhibition with surfactant inhibitors, the critical micelle concentration (CMC) is the most important parameter. When the concentration of surfactant adsorbed on the solid surface is high enough, organized structures (hemimicelles such as bi-or multilayer) are formed, which decrease the corrosion reaction by blocking the metallic surface [13–15].

The aim of this study is to investigate the adsorption and corrosion inhibitive properties of newly synthesized surfactants from the type of fatty acids on mild steel in CO₂-saturated 1% NaCl solution using linear polarization resistance corrosion rate and polarization techniques. Thermodynamic parameters of were determined and the inhibition mechanism has been discussed.

2. Experimental work

A. Chemical composition of mild steel alloy

The rotating disk working electrodes for tests were made of carbon steel grade 080A15 and have an area of 4.55 cm² with a chemical composition (wt%) C 0.18%, Si 0.17%, Mn 0.70%, P 0.011%, S 0.03%, Ni 0.0%, Cr 0.01% and Fe balance. The data was provided by European Corrosion Supplies Ltd.

B. Synthesis of Surfactants

Corn oil was reacted with diethanolamine for 7 hours at 150-160 °C. These processes produce fatty acid diethanolamine amide. Based on the last prepared compound sulfating syntheses were performed. The product is sulfated fatty acid diethanolamine amide. Five types from surfactants were synthesized in high purity by the following compositions: $[R-CH-(OSO_3M)-CON-(CH_2-CH_2-OH)_2]$ (where $M = Na, K, NH_4, -NH-CH_2-CH_2-OH$ and $-N-(CH_2-CH_2-OH)_2$). List of the synthesized surfactants are shown in Table 1.

C. Preparation of solutions

The aggressive solution, 1% NaCl, was prepared by dissolving of analytical grade NaCl in distilled water. The concentration range of the prepared surfactants was from 10 to 75 ppm used for corrosion measurements. All inhibitors solutions were prepared using a mixture from distilled water and alcohol in a different ratio.

D. Corrosion measurements

The measurements were performed on the rotating cylinder electrode ($A=4.55$ cm²). This electrode was used for one time. The reference electrode was Ag/AgCl Electrode to which all potentials are referred. Before beginning the experiment, the prepared 1% - of sodium chloride solution was stirred by a magnetic stirrer for 30 min in 1000 ml cell. Then this cell was thermostated at a temperature 50 ° C for 1 hour under a pressure of 0.9 bars. The solution was saturated with carbon dioxide. To remove any surface contamination and air formed oxide, the working electrode was kept at -1500 mV (Ag/AgCl) for 5 min in the tested

solution, disconnected shaken free of adsorbed hydrogen bubbles and then cathodic and anodic polarization was recorded. ACM Gill AC instrument connected with a personal computer was used for the measurements.

1) The extrapolation of cathodic and anodic Tafel lines

The extrapolation of cathodic and anodic Tafel lines was carried out in a potential range ± 100 mV with respect to corrosion potential (E_{corr}) at scan rate of 1 mV/s.

2) Linear polarization resistance corrosion rate

The linear polarization resistance (LPR) corrosion rate bubble-test method involves evaluating the corrosion of steel in simulated brine saturated with CO_2 at a temperature equivalent to that in the field. The LPR method is ideal for plant monitoring offering an almost instantaneous indication of corrosion rate, allowing for quick evaluation of remedial action and minimizing unscheduled downtime. The potential of the working electrode was varied by a CoreRunning programme (Version 5.1.3.) through an ACM instrument Gill AC. The CoreRunning programme converts a corrosion current in mA/cm^2 to a corrosion rate in mm/year. A cylindrical mild steel rod of the composition 080A15 GRADE STEEL was used as a working electrode. Gill AC technology allows measure DC and AC signals using standard Sequencer software. A small sweep from typically -10 mV to $+10$ mV at 10 mV/min around the rest potential is performed.

E. Surface tension measurements

It is of interest to study the micellar properties of solutions of these compounds in order to correlate their surface active properties with critical micelle concentration (CMC). The surface tensions were determined by DuNouy Tensiometer, Kruss Type 8451 and the temperature was maintained precisely at 25 °C. Critical micelle concentration (CMC) values of surfactants were determined, according to the break points in the plots of the surface tension versus \ln molar concentration of investigated surfactants.

Table 1: list of the synthesized surfactants includes, code number, name and structure.

Code number of the inhibitor	Name and abbreviation	Structure	molecular weight (g /mol)
I	Sodium salt of sulfated fatty acid diethanolamine amide (SS)	$\text{R}-(\text{CH}_2)_8-\text{CH}(\text{CH}_2)_7-\text{C}(\text{O})-\text{N}(\text{CH}_2\text{CH}_2\text{OH})_2$ $\text{O}-\text{S}(=\text{O})_2-\text{ONa}^+$	445

II	Potassium salt of sulfated fatty acid diethanolamine amide (PS)	$\text{R-(CH}_2\text{)}_8\text{-CH-(CH}_2\text{)}_7\text{-C(=O)-N(CH}_2\text{CH}_2\text{OH)}_2\text{-O-SO}_2\text{O}^- \text{K}^+$	461
III	Ammonium salt of sulfated fatty acid diethanolamine amide (AS)	$\text{R-(CH}_2\text{)}_8\text{-CH-(CH}_2\text{)}_7\text{-C(=O)-N(CH}_2\text{CH}_2\text{OH)}_2\text{-O-SO}_2\text{O}^- \text{NH}_4^+$	439
IV	Sulfated fatty acid diethanolamine amide- monoethanolamine complex (MC)	$\text{R-(CH}_2\text{)}_8\text{-CH-(CH}_2\text{)}_7\text{-C(=O)-N(CH}_2\text{CH}_2\text{OH)}_2\text{-O-SO}_2\text{O}^- \text{NH}_3^+\text{-CH}_2\text{CH}_2\text{-OH}$	471
V	Sulfated fatty acid diethanolamine amide- diethanolamine Complex (DC)	$\text{R-(CH}_2\text{)}_8\text{-CH-(CH}_2\text{)}_7\text{-C(=O)-N(CH}_2\text{CH}_2\text{OH)}_2\text{-O-SO}_2\text{O}^- \text{NH}_2^+\text{-(CH}_2\text{CH}_2\text{-OH)}_2$	520

3. Results and Discussion

A. The extrapolation of cathodic and anodic Tafel lines

The inhibiting effect of the synthesized compounds on the corrosion reaction of mild steel in CO_2 -saturated NaCl solution was investigated using the electrochemical polarization method. The polarization technique was adopted to determine both cathodic and anodic polarization curves. It is also used to calculate the corrosion currents from the extrapolation of Tafel lines to pre-determined open circuit potential. This is achieved by measuring the potential–current characteristics of the metal/solution system under consideration with the aid of a potentiostat.

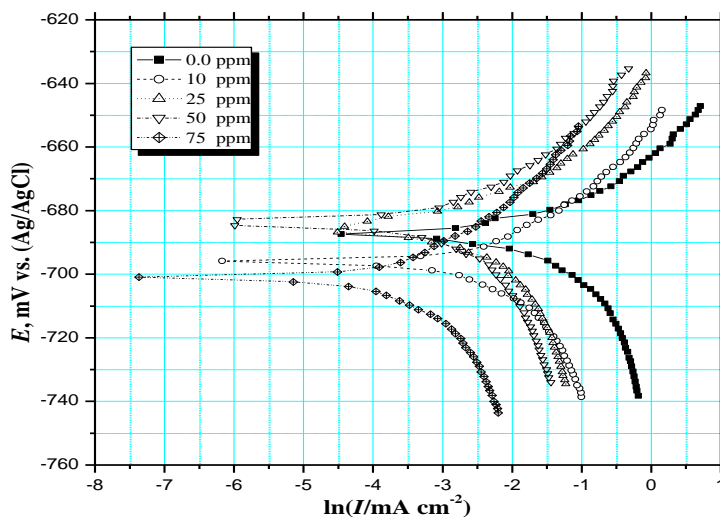


Figure 1: Tafel polarization curves for mild steel in CO_2 -saturated 1% NaCl solution containing different concentration of inhibitor (I) at 50 °C.

Figure 1 shows the influence of inhibitor I concentrations on the Tafel cathodic and anodic polarization characteristics of mild steel in CO₂-saturated solution at scan rate 1 mV/s and at 50 °C. Corrosion parameters were calculated on the basis of cathodic and anodic potential versus current density characteristics in the Tafel potential region [16, 17]. Steady state of open circuit corrosion potential (E_{corr}) for the investigated electrode in the absence and presence of the studied inhibitor was attained after 45–60 min from the moment of immersion. Corrosion current density (I_{corr}) of the investigated electrodes was determined [18], by extrapolation of cathodic and anodic Tafel lines to corrosion potential (E_{corr}). The inhibition efficiency expressed as percent inhibition ($\eta\%$) is defined as:

$$\eta\% = \frac{I_{\text{uninh}} - I_{\text{inh}}}{I_{\text{uninh}}} \times 100 \quad (1)$$

Where I_{uninh} and I_{inh} are the uninhibited and inhibited corrosion currents. The inhibited corrosion currents are those determined in the presence of the studied surfactants used in this investigation. The uninhibited corrosion currents were determined in pure (inhibitor free) CO₂-saturated 1% NaCl solution at the same temperature. It can be seen that the presence of surfactants molecule results a marked shift in both cathodic and anodic branches of the polarization curves towards lower current densities. This means that, the inhibitors affect both cathodic and anodic reactions. It was found that, both anodic and cathodic reactions of mild steel electrode corrosion were inhibited with increasing concentration of synthesized inhibitors. These results suggest that not only the addition of synthesized inhibitors reduce anodic dissolution but also retard the hydrogen evolution reaction.

The electrochemical parameters E_{corr} , I_{corr} , inhibition efficiency ($\eta\%$), anodic and cathodic Tafel slopes (β_a , β_c) obtained from the polarization measurements were listed in Table 2. The data exhibited that, the corrosion current density (I_{corr}) decreases, and the inhibition efficiency ($\eta\%$) increases as the concentration of inhibitors is increased. These results suggest that retardation of the electrodes processes occurs, at both cathodic and anodic sites, as a result of coverage of these sites by surfactants molecules. However, the maximum decrease in I_{corr} was observed for (II) and the inhibition efficiency of the investigated inhibitors was increased in the following order: II > IV > V > I > III at 75 ppm. The increase of inhibitor efficiency with increasing the concentration can be interpreted on the basis of the adsorption amount and the coverage of surfactants molecules, increases with increasing concentration [19, 20]. The E_{corr} values of all synthesized inhibitors were shifted slightly toward both cathodic and anodic directions and did not show any definite trend in CO₂-saturated brine. This may be considered due to the mixed-type behaviour of the studied inhibitors. It can be observed, the shift in E_{corr} that is characteristic of anodic and anodic/cathodic inhibitor [21].

The change in β_a and β_c values as shown in Table 2 indicates that adsorption of synthesized surfactants modify the mechanism of anodic dissolution as well as cathodic hydrogen evolution. In other words, the inhibitor decreases the surface area for corrosion of the investigated metal, and only causes inactivation of a part of the surface with respect to corrosive medium [20]. On the other hand, the cathodic Tafel slopes (β_c) are also found to be greater than the respective anodic Tafel slopes (β_a). These observations are correlated with the fact that the cathodic exchange-current density values are less than those of the anodic counter parts. It can be concluded that the overall kinetics of corrosion of mild steel alloy in CO₂ saturated solution are under cathodic control.

Table 2: Corrosion parameters obtained from Tafel polarization for mild steel in CO₂-saturated solution in the absence and presence of different concentrations of the prepared surfactants at 50 °C.

Inhibitors Code	Conc. of inhibitor (ppm)	$-E_{\text{corr}}$ (mV (Ag/AgCl))	I_{corr} (mAcm ⁻²)	β_a (mVdec ⁻¹)	$-\beta_c$ (mVdec ⁻¹)	θ	$\eta\%$
Absence	0.0	687	0.389	64	117	---	---
I	10	695	0.135	41	95	0.65	65.3
	25	686	0.077	35	96	0.80	80.2
	50	684	0.048	37	100	0.87	87.6
	75	700	0.012	39	98	0.97	96.9
II	10	683	0.055	38	98	0.85	85.8
	25	689	0.013	38	94	0.96	96.6
	50	685	0.005	40	97	0.98	98.7
	75	692	0.002	37	101	0.99	99.4
III	10	692	0.186	38	99	0.52	52.2
	25	686	0.141	42	97	0.63	63.7
	50	683	0.031	38	96	0.92	92.0
	75	685	0.013	36	94	0.97	96.6
IV	10	690	0.081	43	95	0.79	79.1
	25	684	0.042	40	100	0.89	89.2
	50	685	0.027	39	99	0.93	93.0
	75	688	0.009	36	98	0.97	97.6
V	10	688	0.141	35	95	0.63	63.7
	25	690	0.099	37	92	0.74	74.5
	50	682	0.029	39	95	0.92	92.6
	75	694	0.011	40	93	0.97	97.2

B. LPR corrosion rate

Figures 2-4 show that, the change in corrosion rate (CR) with time for mild steel in CO₂-saturated 1%NaCl solution containing different concentrations form inhibitors **I**, **II** and **IV** at 50 °C (as examples). The inhibitor was added after 1 hour of exposure because at this time the corrosion potential got stable, allowing the measurement of the CR prior the injection of the inhibitor. The initial corrosion rate, without inhibitor, was measured to be between 2.59 and 3.784 mm y⁻¹. It can be observed from Figures 5 and 6 that the CR, in the absence of inhibitor, tends to increase with time. The increase in CR has been attributed to the galvanic effect between the ferrite phase and cementite (Fe₃C) which is a part of the original steel in the non-oxidized state and accumulates on the surface after the preferential dissolution of ferrite (α -Fe) into Fe²⁺ [22]. Fe₃C is known to be less active than the ferrite phase. Therefore, there is a preferential dissolution of ferrite over cementite, working the former as the anode and latter as the cathode, favoring the hydrogen evolved reaction (HER) during the corrosion process [23, 24].

Variation of the corrosion rate for inhibitors I, II and IV at different concentrations are presented in Figures 2-4. Corrosion parameters were calculated on the basis of LPR corrosion rate test. The inhibition efficiency ($\eta\%$) and surface coverage (θ) were calculated according to the following equations:

$$\eta\% = \frac{CR_0 - CR_i}{CR_0} \times 100 \quad (2)$$

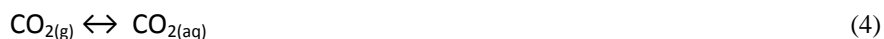
$$\text{Surface coverage } (\theta) = \theta = 1 - \frac{CR_i}{CR_0} \quad (3)$$

Where CR_0 is the corrosion rate without inhibitor and CR_i is the corrosion rate when inhibitor is present. It can be seen that the presence of inhibitors results a high decrease in the rate of corrosion. In the case of these inhibitors, the corrosion rate decreases as the inhibitor concentration increases, getting maximum inhibition efficiency ranged between 61 and 99.5% at 50 ppm after 20 hour of exposure (Table 3). This trend may results from the fact that adsorption and surface coverage increase with the increase in concentration; thus the surface is effectively separated from the medium [25].

Table 3 shows the calculated values of corrosion rates, the inhibition efficiencies and the surface coverage in the absence and presence of different concentrations of different inhibitors at 50 °C. The data exhibited that, the corrosion rates, the inhibition efficiencies and the surface coverage are found to depend on the concentrations of the inhibitors. The corrosion rate (CR) are decreased, and the inhibition efficiencies ($\eta\%$) and the surface coverage (θ) are increased with the increase of the surfactant concentrations. This indicates that the inhibitory action of the inhibitors against mild steel corrosion can be attributed to the adsorption of these molecules on the metal surface, limits the dissolution of mild steel, and the adsorption amounts of surfactants on mild steel increase with concentrations in the corrosive solutions.

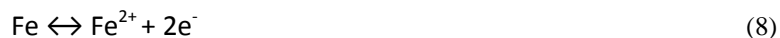
Figure 5 shows the variation of the corrosion rate with time for mild steel in CO_2 -saturated 1% NaCl solution containing 50 ppm from different surfactants at 50 °C. This plot indicates that, the presence of different inhibitors decreases the rate of corrosion. However, the maximum decrease in the corrosion rate was observed for inhibitor (II) and the inhibition efficiency of the investigated surfactants was increased in the following order: II > IV > V > I > III. The inhibition efficiencies are in a good agreement with that calculated from Tafel polarization measurements.

The high inhibition efficiency obtained in CO_2 - saturated solution in the presence of studied inhibitors by all investigated methods can be attributed to the formation of a protective film of iron carbonate (FeCO_3) as follows [26]:





The anodic dissolution for iron in carbonic acid solutions gives ferrous ions [26].



According to these processes, a corrosion layer was formed on the steel surface. The properties of the formed layers and its effect on the corrosion rate are important factors to take into account when studying the corrosion of steels in CO₂ environments. Ogundele and White suggested that, iron carbonate, FeCO₃, may be important in the formation of protective layers on steel surface [27]. The formation of iron carbonate can be explained by using the following Eq.[28].

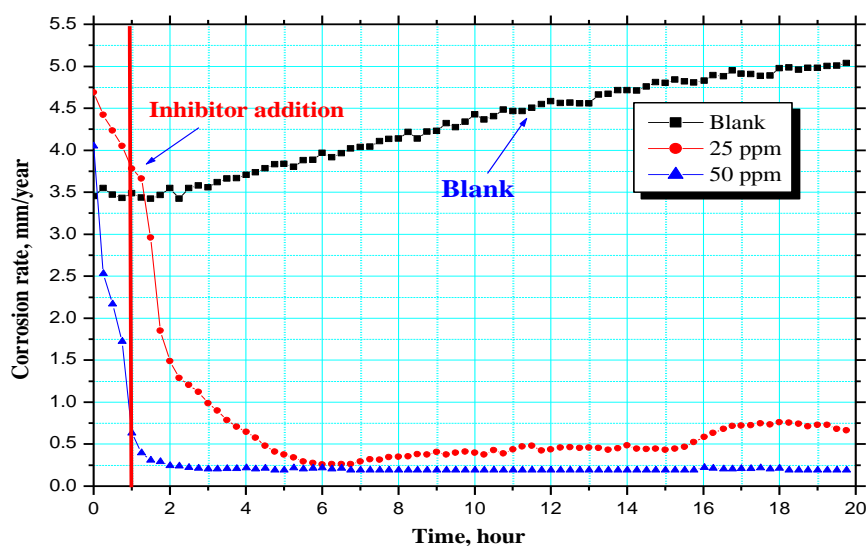


Figure 2: Variation of the Corrosion rate with time for carbon steel in CO₂-1% NaCl solution containing different concentrations of SS at 50 °C.

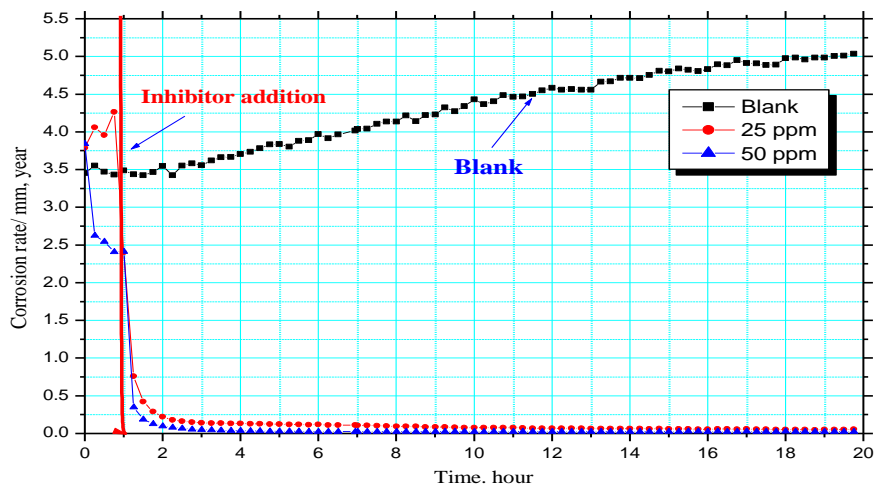


Figure 3: Variation of the Corrosion rate with time for carbon steel in CO₂-1% NaCl solution containing different concentrations of PS at 50 °C.

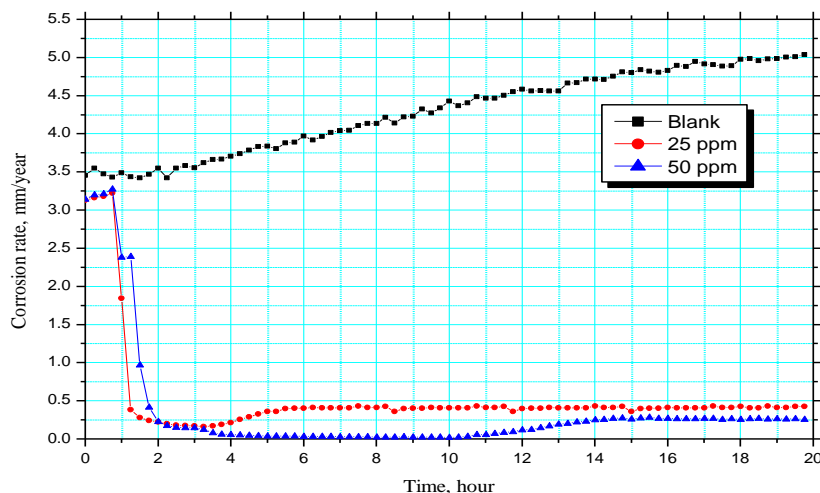


Figure 4: Variation of the Corrosion rate with time for carbon steel in CO₂-1% NaCl solution containing different concentrations of MC at 50 °C.

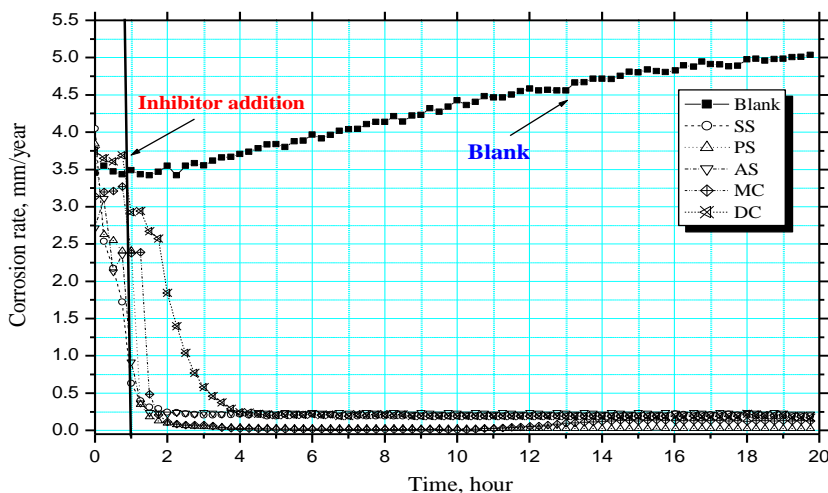


Figure 5: Variation of the Corrosion rate with time for carbon steel in CO₂-1% NaCl solution containing 50 ppm of different inhibitors at 50 °C.

Table 3: The corrosion parameters obtained from LPR corrosion rate measurements for mild steel electrode in CO₂-saturated 1% solution of NaCl in the absence and presence of various concentrations of inhibitors obtained based on corn oil at 50 °C.

Inhibitors	Concentration, ppm	Corrosion rate (mm/year)	Surface coverage θ	The inhibition efficiency, IE%
Absence	0.0	5.0373	-----	-----
SS	25	0.6656	0.87	87
	50	0.1939	0.96	96
PS	25	0.0535	0.99	99
	50	0.0252	0.995	99.5
AS	25	2.001	0.61	61
	50	0.2244	0.95	95.6
MC	25	0.42505	0.92	92
	50	0.25591	0.95	95
DC	25	1.354	0.73	73.5
	50	0.170	0.96	96.6

C. Surface tension and surface active properties

The main importance of the critical micelle concentration (CMC) consists of the fact that at this concentration, most of the physical and chemical properties of the surfactant solutions present an abrupt variation. The values of surface tension (γ) were measured at 303 K for various concentrations of the synthesized surfactants. The measured values of (γ) were plotted against $\ln C$ (Fig. 6). The intercept of the two straight lines designates the CMC, where saturation in the surface adsorbed layer takes place. The plot showed that the surfactant was molecularly dispersed at low concentration leading to a reduction in surface tension. This reduction increases with increasing concentration. At high concentration, however, when a certain concentration was reached (CMC), the surfactant molecules form micelles, which were in equilibrium with the free surfactant molecules [28].

The surface active properties of the surfactant, effectiveness (π_{cmc}), maximum surface excess (Γ_{max}), and minimum area per molecule (A_{min}) were calculated using the following equations [29]:

$$\pi_{\text{cmc}} = \gamma_0 - \gamma_{\text{cmc}} \quad (10)$$

$$\Gamma_{\text{max}} = \frac{-1}{RT[\partial\gamma/\partial\ln C]_T} \quad (11)$$

$$A_{\text{min}} = \frac{1}{\Gamma_{\text{max}} \times N_A} \quad (12)$$

$$\Delta G_{\text{mic}}^{\circ} = RT \ln CMC \quad (13)$$

$$\Delta G_{\text{ads}}^{\circ} = \Delta G_{\text{mic}}^{\circ} - 0.6023\pi_{\text{CMC}}A_{\text{min}} \quad (14)$$

Where $\partial\gamma/\partial\ln C$ is maximum slope, γ_0 is the surface tension of pure water, γ_{cmc} the surface tension at critical micelle concentration, N_A is the Avogadro's number (6.023×10^{23} molecules/mol), R is the molar gas constant ($R = 8.314 \text{ J}/(\text{mol K})$) and T is the absolute temperature ($= (t^{\circ}\text{C} + 273)$), $\Delta G_{\text{mic}}^{\circ}$ is the Gibbs free energy of micellization, $\Delta G_{\text{ads}}^{\circ}$ is the Gibbs free energy of adsorption [30].

The data presented in Table 4 show some of the surface active properties for the investigated surfactants. The results indicate that, the consequent increase in of Γ_{max} leads to crowding at the interface, which causes a decrease in A_{min} values. This is because the minimum surface area decreases with increases in the chain length of the synthesized surfactant molecules. The data on the minimum surface area of the short chain surfactant molecules showed higher A_{min} of these molecules compared to the longer hydrophobic chains [30]. The values of effectiveness (π_{cmc}) at 298 K indicate that the prepared compounds gives large reduction of surface tension at CMC, so that, these compounds acts as effective corrosion inhibitors for carbon steel in CO_2 - saturated 1% NaCl solutions.

The free energy changes of micellization and adsorption showed negative sign showing the spontaneity of the two processes at 25 °C. Moreover, $\Delta G_{\text{ads}}^{\circ}$ increase in negativity than $\Delta G_{\text{mic}}^{\circ}$. That showed the higher

tendency of these surfactants towards adsorption rather than micellization. Then the adsorption will be accompanied with micellization at last. The tendency towards adsorption was referred to the interaction between the aqueous phases and the hydrophobic chains which pump the surfactant molecules to the interface [31].

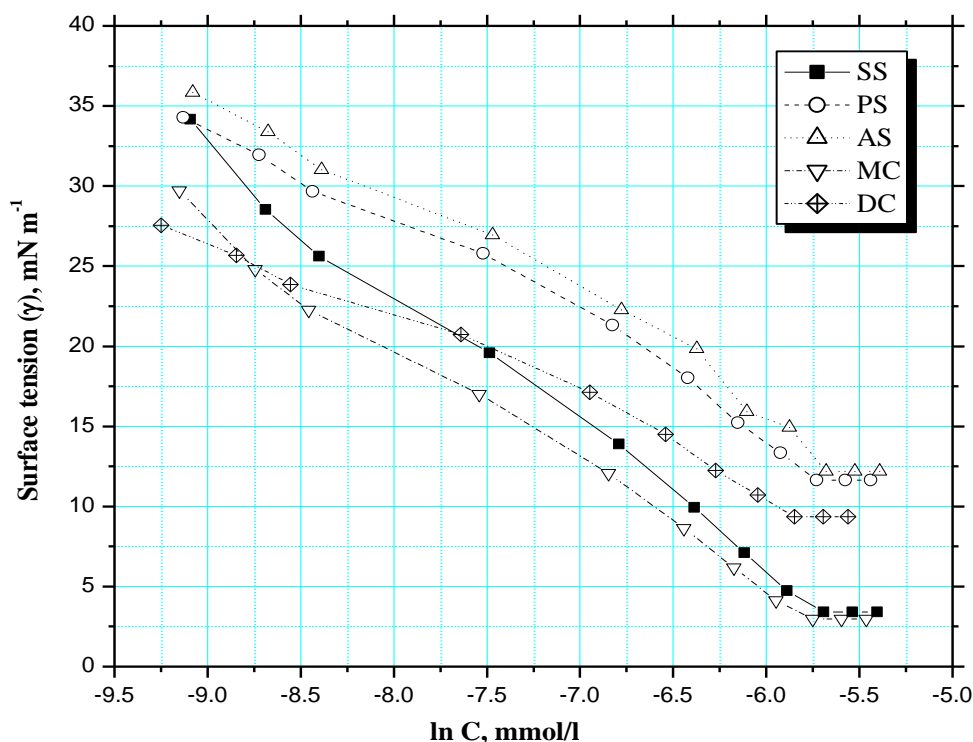


Figure 6: Change of surface tension (γ) with the concentration of the surfactants at 25 °C.

D. Adsorption Isotherm

The mechanism of corrosion inhibition may be explained on the basis of the adsorption behaviour of the inhibitors [32]. The degree of surface coverage (θ) for different inhibitor concentrations was evaluated from polarization measurements by following equation:

Table 4: The critical micelle concentration and surface parameters of the synthesized surfactants.

Inhibitors	CMC (mmol/l) $\times 10^{-3}$	γ_{cmc} (mN m ⁻¹)	π_{cmc} (mN m ⁻¹)	Γ_{max} (mol cm ⁻²) $\times 10^{-10}$	A_{min} (nm ²)	ΔG_{mic}^o kJ/mol	ΔG_{ads}^o kJ/mol
I	3.37	3.42	68.58	4.41	0.37	-25.1	-35.6
II	3.24	11.65	60.35	5.11	0.32	-24.6	-33.9
III	3.41	12.17	59.83	5.57	0.29	-25.6	-35.5
IV	3.10	2.97	69.03	6.18	0.25	-26.1	-37.8
V	2.88	9.36	62.64	7.01	0.23	-26.9	-39.4

$$\theta = \frac{I_{uninh} - I_{inh}}{I_{uninh}} \quad (15)$$

We attempted to fit θ values with standard adsorption isotherms, including those of Frumkin, Flory-Huggins, Temkin, and also by the Langmuir-type adsorption isotherm. It was found that the experimental results for all investigated surfactants can be fitted quite well with the Langmuir adsorption isotherm expressed as [33]:

$$\frac{C_i}{\theta} = \frac{1}{K_{ads}} + C_i \quad (16)$$

Where C_i is the inhibitor concentration and K_{ads} is the equilibrium constant of the inhibitor adsorption process related to the free energy of adsorption ΔG_{ads}^o by

$$K_{ads} = \frac{1}{55.5} \exp\left(-\frac{\Delta G_{ads}^o}{RT}\right) \quad (17)$$

The value 55.5 in the above equation was the molar concentration of water in solution in mol/L. Plotting C_i / θ vs. C_i yielded a straight line (Fig. 7) with a correlation coefficient (R^2) higher than 0.9976 and a slope closed to the unity. This indicates that the adsorption of these inhibitors can be fitted to a Langmuir adsorption isotherm. The strong correlation of the Langmuir adsorption isotherm may confirm the validity of this approach. The equilibrium constant (K_{ads}) for the adsorption-desorption process of these compounds can be calculated from reciprocal of the intercept. The adsorptive equilibrium constant (K_{ads}) values are listed in Table 5. It is clear that, the high values of K_{ads} suggest that interaction between adsorbed molecules and the metal surface is strong, indicating that the inhibitor molecules are not easily removable from the surface by the solvent molecules. This may be due to the formation of coordinated bonds between the prepared surfactants and the d-orbital of iron on the surface of mild steel.

Generally, values ΔG_{ads}^o around -20 kJ mol^{-1} or lower are consistent with the electrostatic interaction between the charged molecules and the charged metal (physisorption). Whereas, the more negative values than -40 kJ mol^{-1} involve charge sharing or transfer from the inhibitor molecules to the metal surface to form a coordinate type of bond (chemisorption) [35]. In our measurements, calculated ΔG_{ads}^o values indicated that the adsorption mechanism of the prepared surfactants on mild steel in CO_2 -saturated 1% NaCl solution is a physical adsorption [36].

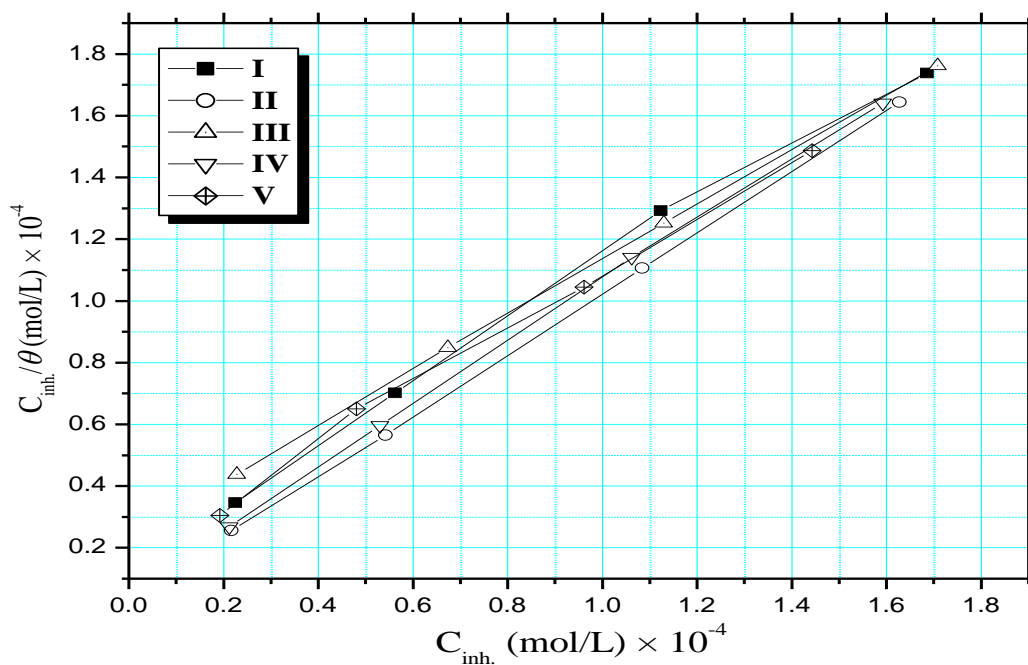


Figure 7: Langmuir adsorption isotherm (C_{inh}/θ vs. C_{inh}) fitting of the obtained from polarization measurements for mild steel in CO_2 saturated 1% NaCl solution containing various concentrations of inhibitors at 50°C .

Table 5: Thermodynamic parameters for the adsorption of the studied surfactants on mild steel electrode in CO_2 - saturated 1% NaCl solutions

Inhibitors	Slope	Regression coefficients, R^2	$K_{ads}, \text{M}^{-1} \times 10^4$	ΔG_{ads}^o (KJ mol $^{-1}$)
I	1.021	0.9976	1.260	-14.61
II	1.115	0.9999	1.315	-14.72
III	1.021	0.9999	1.190	-14.45
IV	1.013	0.9997	1.061	-14.15
V	1.010	0.9979	1.221	-14.52

4. Conclusions

In the above results and discussion, the following conclusions are drawn:

1. Novel environmental friendly surfactants from the type of fatty acids were synthesized based on corn oil and diethanolamine.

2. Synthesized surfactants acts as a good inhibitor for the corrosion of mild-steel in CO₂ saturated solutions, and the maximum inhibition efficiency is about 99.5% for PS inhibitor.
3. Inhibition efficiency increases with increasing surfactant concentration. Maximum inhibition efficiencies were observed at 75 ppm.
4. The LPR corrosion rate and the electrochemical polarization studies are in good agreement. Surfactants act as a mixed-type inhibitor in CO₂ environments.
5. The surface activity of the synthesized surfactants solutions was determined using surface tension measurements at 25 °C.
6. The adsorption of inhibitors on mild steel surface obeys the Langmuir adsorption isotherm. Physisorption is proposed as the mechanism for corrosion inhibition.

References

- [1] A. Yildirim, M. Cetin, Synthesis and evaluation of new long alkyl side chainacetamide, isoxazolidine and isoxazoline derivatives as corrosion inhibitors, *Corros. Sci.* **50**, p. 155–165, 2008.
- [2] E.E. Oguzie, Y. Li, F.H. Wang, Corrosion inhibition and adsorption behavior of methionine on mild steel in sulfuric acid and synergistic effect of iodide ion, *J. Colloid Interface Sci.* **310**, p. 90–98, 2007.
- [3] A. Fiala, A. Chibani, A. Darchen, A. Boulkamh, K. Djebbar, Investigations of the inhibition of copper corrosion in nitric acid solutions by ketene dithioacetal derivatives, *Appl. Surf. Sci.* **253**, p. 9347–9356, 2007.
- [4] I.B. Obot, N.O. Obi-Egbedi, S.A. Umoren, The synergistic inhibitive effect and some quantum chemical parameters of 2,3-diaminonaphthalene and iodide ions on the hydrochloric acid corrosion of aluminium, *Corros. Sci.* **51**, pp. 276–282, 2009.
- [5] M. El Achouri, S. Kertit, H.M. Gouttaya, B. Nciri, Y. Bensouda, L. Perez, M.R. Infante, K. Elkacemi, Corrosion inhibition of iron in 1M HCl by some gemini surfactants in the series of alkanediyl-*l,l'*-bis-(dimethyl tetradecyl ammonium bromide), *Proc. Org. Coat.* **43**, p. 267–273, 2001.
- [6] T.P. Zhao, G.N. Mu, The adsorption and corrosion inhibition of anion surfactants on aluminium surface in hydrochloric acid, *Corros. Sci.* **41**, p.1937–1944, 1999.
- [7] V. Branzoi, F. Branzoi, M. Baibarac, The inhibition of the corrosion of Armco iron in HCl solutions in the presence of surfactants of the type of N-alkyl quaternary ammonium salts, *Mater. Chem. Phys.* **65**, p. 288–297, 2000.
- [8] R. Guo, T.Q. Liu, X. Wei, Effects of SDS and some alcohols on the inhibition efficiency of corrosion for nickel, *Colloids Surf. A* **209**, p. 37–45, 2002.
- [9] J.M. Bastidas, P. Pinilla, J.L. Polo, S. Miguel, *Corros. Sci.* **45**, p. 427, 2003.
- [10] A.E. Bolzán, I.B. Wakenge, R.C.V. Piatti, R.C. Salvarezza, A.J. Arvia, *J. Electroanal. Chem.* **501**, p. 241, 2001.
- [11] E. Stipnišek-Lisac, A. Gazivoda, M. Madžarac, *Electrochim. Acta* **47**, p. 4189, 2002.
- [12] M. Sahin, S. Bilgic, H. Yilmaz, *Appl. Surf. Sci.* **195**, p. 1, 2002.
- [13] M. Houyi, C. Shenhao, Y. Bingsheng, Z. Shiyong, L. Xiangqian, *Corros. Sci.* **45**, p. 867, 2003.
- [14] M.L. Free, *Corros. Sci.* **44**, p. 2865, 2002.
- [15] M.L. Free, *Corrosion* **58**, p. 1025, 2002.
- [16] R. Tremont, H. De Jesus-Cardona, J. Garcia-Orozco, R.J. Castro, C.R. Cabrera, 3-Mercaptopropyltrimethoxysilane as a Cu corrosion inhibitor in KCl solution, *J. Appl. Electrochem.* **30**, p. 737-743, 2000.
- [17] J.W. Schultze, K. Wippermann, Inhibition of Electrode processes on copper by AHT in acid solution *Electrochim. Acta*, **32**, p. 823-831, 1987.
- [18] A. El-Sayed, H. S. Mohran, Hany M. Abd El-Lateef, Inhibitive action of ferricyanide complex anion on both corrosion and passivation of zinc and zinc–nickel alloy in the alkaline solution, *Journal of Power Sources* **196**, p. 6573–6582, 2011.
- [19] E. Akbarzadeh, M. N. M. Ibrahim, A. A. Rahim, Corrosion Inhibition of Mild Steel in Near Neutral Solution by Kraft and Soda Lignins Extracted from Oil Palm Empty Fruit Bunch, *Int. J. Electrochem. Sci.*, **6**, p. 5396 – 5416, 2011.
- [20] A. El-Sayed, Hossnia S. Mohran, H.M. Abd El-Lateef, The inhibition effect of 2,4,6-tris (2-pyridyl)-1,3,5-triazine on corrosion of tin, indium and tin–indium alloys in hydrochloric acid solution *Corros. Sci.* **52**, p. 1976–1984, 2010.
- [21] D. A. López, S. N. Simison, S. R. de Sánchez, *Corr. Sci.* **47**, p. 735-775, 2005.
- [22] N. Staicopolus, *J. Electrochem. Soc.* **110**, p. 1121-1124, 1963.

- [23] J. Crolet, N. Thevenot, S. Nestic, *Corrosion*, **54**, 194-203, 1998.
- [24] K. Videm, J. Kvarekvaal, T. Perez, G. Fitzsimons, NACE Corrosion/96, Houston, Texas, 1996, Paper No. 1.
- [25] A. El-Sayed, A. M. Shaker, H. M. Abd El-Lateef, Corrosion inhibition of tin, indium and tin–indium alloys by adenine or adenosine in hydrochloric acid solution, *Corros. Sci.* **52**, 72-81, 2010.
- [26] Damia'n A. Lo'pez, S.N. Simison, S.R. de Sa'nchez, The influence of steel microstructure on CO₂ corrosion. EIS studies on the inhibition efficiency of benzimidazole, *Electrochimica Acta* **48**, p. 845- 854, 2003.
- [27] G.I. Ogundele, W.E. White, *Corrosion* **42**, p.71, 1986.
- [28] M. A. Migahed, M. Abd-El-Raouf, A. M. Al-Sabagh, H. M. Abd-El-Bary, *J. Appl. Electrochem.*, **36**, 395, 2006.
- [29] M. J. Rosen, *Surfactants and Interfacial Phenomena*, John Wiley and Sons Inc., New York, 1978.
- [30] A.M. Badawi, M. A.S. Mohamed , M.Z. Mohamed, M.M. Khowdairy, Surface and antitumor activity of some novel metal-based cationic surfactants, *J Cancer Res Ther*, **3**, p. 198-206, 2007.
- [31] A.M. Alsabagh , M.A. Migahed, Hayam S. Awad, Reactivity of polyester aliphatic amine surfactants as corrosion inhibitors for carbon steel in formation water (deep well water), *Corro. Sci.* **48**, p. 813–828, 2006.
- [32] M.A. Quraisi, A.S. Mideen, M.A.W. Khan, M. Ajmal, *Indian J. Chem. Technol.* **1**, p. 329, 1994.
- [33] M.A. Hegazy, H.M. Ahmed, A.S. El-Tabei, Investigation of the inhibitive effect of p-substituted 4-(N,N,N-dimethyldodecylammonium bromide)benzylidene-benzene-2-yl-amine on corrosion of carbon steel pipelines in acidic medium, *Corro. Sci.*, **53**, p. 671–678, 2011.
- [34] S.M.A. Hosseini, A. Azimi, *Corros. Sci.* **51**, p. 728–832, 2009.
- [35] P.C. Okafor, Yugui Zheng, *Corros. Sci.* **51**, p. 850–859, 2009.
- [36] M. Behpour, S.M. Ghoreishi, N. Soltani, M. Salavati-Niasari, M. Hamadianian, A. Gandomi, *Corros. Sci.* **50**, p.2173–2182, 2008